

## Elongational flow opto-rheometry for polymeric liquids: 4. Rayleigh scattering studies on elongational flow-induced crystallization of poly(ethylene terephthalate) in the supercooled state

Hiroshi Kubo, Harumi Sato, Masami Okamoto and Tadao Kotaka\*

Advanced Polymeric Materials Engineering, Graduate School of Engineering, Toyota  
 Technological Institute, Hisakata 2-12-1, Tempaku, Nagoya 468, Japan  
 (Revised 2 April 1997)

Rayleigh scattering studies were conducted in order to examine the elongational flow-induced crystallization behaviour of poly(ethylene terephthalate) (PET) in the supercooled liquid state (100–130°C). In the specimen elongated at 110°C where spherulite growth was negligible, initially nothing happened, but flow-induced crystallization then occurred rather suddenly at a critical tensile strain of  $\epsilon (= \dot{\epsilon}_0 t) \approx 2$  in Hencky units, independent of the strain rate  $\dot{\epsilon}_0$ . At this temperature the  $H_v$  (cross-polarized) scattering yielded two-point patterns parallel to the elongational direction with strong streaks in the perpendicular direction. The result implies that molecular orientation proceeded along the flow direction and the crystalline domain grew transverse to the oriented chains. In contrast, at 130°C, especially with low  $\dot{\epsilon}_0$ , where spherulite growth was rapid, a four-leaf-clover pattern typical of spherulites was observed at the start of elongation  $\epsilon = 0$ . In the following stages, spherulite growth surpassed the destruction of existing spherulites and/or flow-induced oriented crystallite formation, and a smeared four-leaf-clover pattern was thus observed even at a level of  $\epsilon = 1.3$ . © 1997 Elsevier Science Ltd.

(Keywords: elongational flow; induced crystallization; poly(ethylene terephthalate))

### Introduction

In our previous paper<sup>1</sup>, we described the elongational flow-induced crystallization behaviour of poly(ethylene terephthalate) (PET) studied via elongational flow opto-rheometry (EFOR)<sup>2,3</sup> in supercooled liquid states in the temperature range 100–130°C, comparable with blow moulding and/or film blowing conditions for PET<sup>4–10</sup>. We specifically discussed the influence of spherulite and/or flow-induced oriented crystalline formation on the transient elongational viscosity  $\eta_E(t)$  and birefringence  $\Delta n(t)$  based on the combined results of EFOR and temperature-modulated differential scanning calorimetry (TMDSC) (see, for example, Ref. 11) and also of the observation of spherulite growth behaviour of PET in quiescent states in the same temperature range. The main features of our observation were as follows<sup>1</sup>. At high temperatures (around 130°C) especially with low  $\dot{\epsilon}_0$  (less than  $0.1 \text{ s}^{-1}$ ) where spherulite growth was rapid,  $\eta_E(t)$  exhibited a change from a slow to a rapid increase with time  $t$  at a certain critical strain that we called the ‘up-rising’ strain  $\epsilon_{\eta_E} (= \dot{\epsilon}_0 t_{\eta_E}) \approx 0.5$  in Hencky units, independent of the strain rate  $\dot{\epsilon}_0$ . The degree of crystallinity increased constantly with  $\epsilon(t) = \dot{\epsilon}_0 t$  and reached as much as 11.2% at  $\epsilon(t) \approx 1.3$ . On the other hand, at low temperature (around 110°C) where spherulite growth was negligible, the degree of crystallinity stayed almost zero up to around  $\epsilon(t) \approx 1.6$ , beyond which it increased rapidly<sup>1</sup>. EFOR studies combined with TMDSC revealed that flow-induced crystallization appeared to have taken place in the elongated specimens beyond  $\epsilon(t) \equiv \epsilon_{\Delta n} \approx 1.6$ , again independent of  $\dot{\epsilon}_0$ .

However, the above interpretation was temporary, based partly on speculation derived from observation of the crystallization behaviour of PET in quiescent states<sup>1</sup>. For a

better understanding of the development of the morphology, one needs to pin down the morphological details of the developed structure by carrying out a quantitative structural analysis such as by light scattering. The main aim of this communication is thus to correlate the complex  $\eta_E(t)$  and/or  $\Delta n(t)$  versus  $t$  profiles with the developed internal structures at the submicrometer level. We present here some preliminary results of typical Rayleigh scattering patterns obtained on supercooled PET specimens under transient elongational flow.

### Experimental

The details of the EFOR and TMDSC runs were described elsewhere<sup>1,2</sup>. Here we briefly describe the light scattering method added for this experiment. For the light scattering studies, a test specimen subjected to EFOR to a certain extent of elongation  $\epsilon(t)$  was quickly quenched by sandwiching it between cold metal plates in order to freeze the internal structure developed during the elongation. The centre of the specimen was cut out and used for later scattering measurements.

Polarized He–Ne laser light of 632.8 nm wavelength was applied (at an ambient temperature) vertically to the stretched direction of the elongated specimen, thickness about 40–200  $\mu\text{m}$ , held between cover glasses to avoid a diffuse surface. The scattering pattern under  $H_v$  (cross-polarized) optical alignment was recorded on a photographic film (Fuji FP-100B; ISO = 100) with an exposure time of 1–1/4 s. The distance between the sample and the film was 85.0 mm, which gave a scattering vector range of around  $0.37\text{--}7.00 \mu\text{m}^{-1}$ .

### Results and discussion

Figure 1a shows a typical example of the variation of the tensile stress  $\sigma(t)$  versus Hencky strain  $\epsilon (= \dot{\epsilon}_0 t)$  elongated

\* To whom correspondence should be addressed

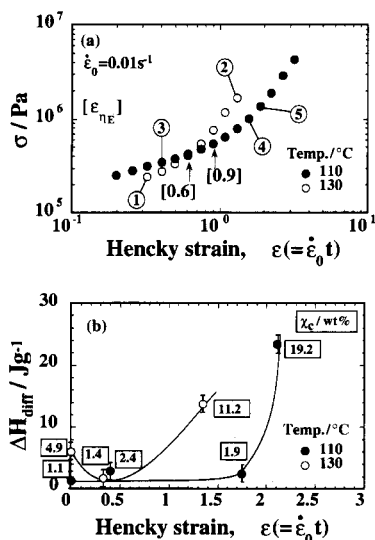


**Figure 1** (a) Double logarithmic plots of tensile stress  $\sigma$  versus Hencky strain  $\epsilon (= \dot{\epsilon}_0 t)$  and (b) heat flow difference  $\Delta H_{diff}$  versus  $\epsilon$  (Fig. 8 of our previous paper<sup>1</sup>) at 110 and 130°C with  $\dot{\epsilon}_0 = 0.01 \text{ s}^{-1}$ . The arrows in (a) indicate the critical Hencky strain  $\epsilon_{\eta E}$  at which the upward deviation of  $\eta_E(\epsilon)$  takes place. The attached numbers in (a) correspond to scattering patterns shown in Figure 2

(after  $\epsilon_{\eta E}$ ) is rather rapid, while at 130°C the tendency is the opposite, so that these curves exhibit a more gradual change than the 110°C curves. We notice here that the upward deviation of the  $\sigma(t)$  versus  $\epsilon(t)$  curves takes place around  $\epsilon_{\eta E} = 0.9$  in Hencky units at 110°C and  $\epsilon_{\eta E} = 0.6$  for 130°C as indicated by the upward arrows in the figure. At 110°C the influence of spherulite formation on the deviation of  $\sigma(t)$  is rather small so that  $\epsilon_{\eta E}$  is almost constant (around 1) against  $\dot{\epsilon}_0$ . This trend resembles the features of usual molten polymer elongation such as for polystyrene and polyethylene<sup>2,3</sup>. At 130°C, however, spherulite growth may take place dominantly so that  $\epsilon_{\eta E}$  (less than 1) is small especially in the specimen elongated with low  $\dot{\epsilon}_0$ .

Figure 2 shows light scattering patterns corresponding to the specimens marked in Figure 1 by the numbers in circles. We see several interesting features of the developed internal structures from the light scattering patterns obtained at 110°C and at 130°C as shown in Figure 2. We observe weak scattering with a slight anisotropy from the specimen at 130°C before the start of elongation  $\epsilon = 0$ . Because of the 90 s idle time before the start, spherulite formation started in this specimen and reached 4.9 wt.% crystallinity, as revealed by TMDSC analysis<sup>1</sup>. The spherulites continued to grow and a four-leaf-clover pattern is seen at an

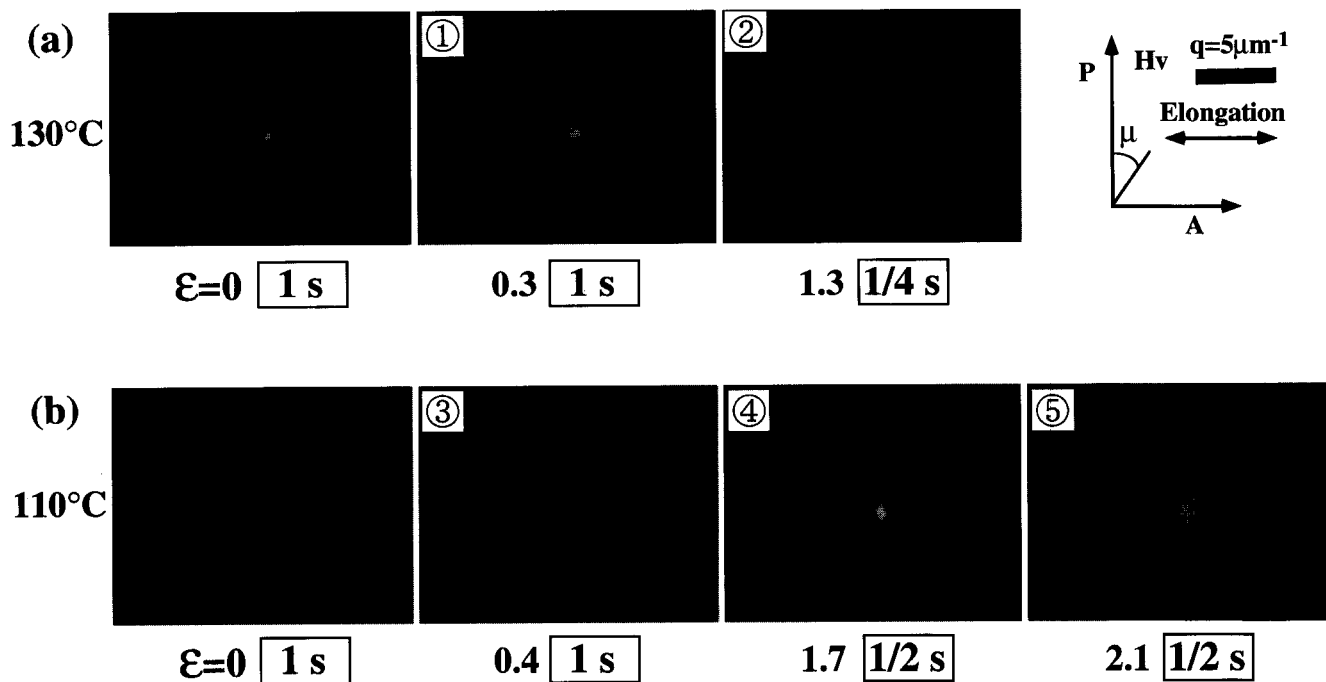


**Figure 2**  $H_v$  scattering patterns for the specimens of various Hencky strain  $\epsilon$  at (a) 130°C and (b) 110°C with  $\dot{\epsilon}_0 = 0.01 \text{ s}^{-1}$ . The analyzer is parallel to the elongational direction. The number in the circle for each photograph corresponds to the number in Figure 1a. The exposure time is shown by the number in the box

with  $\dot{\epsilon}_0 = 0.01 \text{ s}^{-1}$  in the supercooled state at 110 and 130°C, and Figure 1b is a reproduction of Fig. 8 of our previous paper<sup>1</sup> showing the variation of the enthalpy of crystalline melting (corresponding to the degree of crystallinity) of the elongated specimens. As seen in Figure 1a and also discussed previously<sup>1</sup>, the shapes or the curvatures of the  $\sigma(t)$  versus  $\epsilon(t)$  curves obtained at 110°C differ from those obtained at 130°C. In the former, the rate of increase in the linear portion (before the ‘up-rising’ at  $\epsilon_{\eta E} (= \dot{\epsilon}_0 t_{\eta E})$ ) of the curves is rather slow but that in the non-linear portion

elongation of  $\epsilon = 0$  as well as at a high elongation of  $\epsilon = 1.3$  (stretch ratio  $\lambda$  of around 3.7), in which the pattern becomes smeared but with increasing intensities. This is typical of scattering patterns from growing spherulites. The spherulite growth took place even in the liquid under elongation. The structural growth was slightly disturbed on elongation, but substantial deformation of the grown spherulites had not occurred, as judged from the apparently constant azimuthal angle  $\mu$  (about 45°) with the maximum intensity.

On the other hand, in the specimen elongated at 110°C, a strong streak appears at  $\epsilon = 1.7$  ( $\lambda$  about 5.5) around the meridional direction perpendicular to the stretch direction, suggesting that strong molecular orientation proceeded around the elongational direction in real space. Furthermore, at  $\epsilon = 2.1$ , two-strong-spot-like scattering appears around the horizontal direction parallel to the stretch direction. Another interesting feature is that the appearance of the two-spot-like pattern at around  $\epsilon = 2.0$  agrees well with the evidence that the percentage crystallinity of the elongated specimen abruptly increased at around  $\epsilon = 2.0$  as revealed by TMSCA analysis. Our EFOR analysis<sup>1</sup> showed that the  $\Delta n(\epsilon)$  versus  $\epsilon$  curve deviated upward at an (up-rising) Hencky strain  $\epsilon_{\Delta n}$  of approximately 2, where the percentage crystallinity of the specimen reached 19.2 wt.%<sup>1</sup>. The strong two-spot pattern is presumably a proof of elongational flow-induced oriented-crystallite formation. Under a depolarized optical alignment ( $V_v$ ), the same scattering pattern was obtained. These results imply that the crystalline texture grows essentially normal to the oriented chain, i.e. lateral growth of the crystallites proceeded with elongation. Recently, Göschel and Urban reported from their small-angle X-ray scattering studies<sup>12</sup> that a uniaxially oriented PET film shows a typical two-point pattern, which is caused by stacked lamellae formation, in which the lamellae normal coincide with the drawing direction. A structure having the same crystalline texture has presumably developed in our PET specimen elongated at 110°C. The influence of  $\Delta n$  on the scattering intensity is generally not negligible<sup>13,14</sup>, but in our case it is very small because the elongational direction is parallel to

the analyzer. We estimated roughly the scale as being 1.5–2  $\mu\text{m}$  from the long period of the crystalline domains corresponding to a maximum peak of the spots at  $\epsilon = 2.1$ .

In the light scattering pattern for the specimen elongated up to  $\epsilon = 2.1$  at 110°C, a clear two-point pattern was observed, which is quite reasonable and represents nicely a feature of elongational flow-induced crystallization. By the above approaches we can correlate the elongational flow behaviour of supercooled PET liquids with the internal structure developed during elongational flow. A complete analysis of the results and more detailed data will be published later.

#### References

1. Okamoto, M., Kubo, H. and Kotaka, T., *Polymer*, 1997, in press.
2. Kotaka, T., Kojima, A. and Okamoto, M., *Rheol. Acta*, 1997, in press.
3. Okamoto, M., Kojima, A. and Kotaka, T., *Polymer*, 1997, in press.
4. Radhakrishnan, J. and Gupta, V.B.J., *Macromol. Sci.-Phys.*, 1993, **B32**, 243.
5. Jabarin, S.A., *Polym. Eng. Sci.*, 1992, **32**, 1341.
6. Salem, D.R., *Polymer*, 1994, **35**, 771.
7. Lorentz, G. and Tassin, J.F., *Polymer*, 1994, **35**, 3200.
8. Huang, B., Ito, M. and Kanamoto, T., *Polymer*, 1994, **35**, 1210.
9. Lofgren, E.A. and Jabarin, S.A., *J. Appl. Polym. Sci.*, 1994, **51**, 1251.
10. Cole, K.C., Guévremont, J., Aji, A. and Dumoulin, M.M., *Appl. Spectrosc.*, 1994, **48**, 1513.
11. Sauerbrunn, S. and Gill, P., *Am. Lab.*, 1993, **25**, 54.
12. Göschel, U. and Urban, G., *Polymer*, 1995, **36**, 3633.
13. Hashimoto, T., Nagatoshi, K. and Kawai, H., *Polymer*, 1976, **17**, 1075.
14. Matsuo, M., Ozaki, F., Kurita, H., Sugawara, S. and Ogita, T., *Macromolecules*, 1980, **13**, 1187.